INVESTIGATING iRHOM2-ASSOCIATED TRANSCRIPTIONAL CHANGES IN TYLOSIS WITH ESOPHAGEAL CANCER

Stephen Murtough, Deepak Babu, Catherine M. Webb, Hélène Louis dit Picard, Lisa A. McGinty, Jennifer Chao-Chu, Ryan Pink, Andrew R. Silver, Howard L. Smart, John K. Field, Philip Woodland, Janet M. Risk, Diana C. Blaydon, Daniel J. Pennington, David P. Kelsell

PII: S2772-5723(23)00203-0

DOI: https://doi.org/10.1016/j.gastha.2023.12.007

Reference: GASTHA 412

To appear in: *Gastro Hep Advances*

Received Date: 14 February 2023

Revised Date: 19 December 2023

Accepted Date: 19 December 2023

INVESTIGATING iRHOM2-ASSOCIATED TRANSCRIPTIONAL CHANGES IN TYLOSIS WITH ESOPHAGEAL CANCER

AUTHORS AND AFFILIATIONS

Stephen Murtough[1], Deepak Babu[1], Catherine M. Webb[1], Hélène Louis dit Picard[1], Lisa A. M^{c}Ginty[1], Jennifer Chao-Chu[1], Ryan Pink[2], Andrew R. Silver[1], Howard L. Smart[3], John K. Field[4], Philip Woodland[5], Janet M. Risk[4], Diana C. Blaydon[1], Daniel J. Pennington[1], David P. Kelsell[1]

[1]Blizard Institute, Faculty of Medicine and Dentistry, Queen Mary University of London, London, UK

[2]Department of Biological and Medical Sciences, Faculty of Health and Life Sciences, Oxford Brookes University, Oxford, UK

[3]Liverpool University Hospitals NHS Foundation Trust, Liverpool, UK

[4]Department of Molecular and Clinical Cancer Medicine, Institute of Systems, Molecular and Integrative Biology, University of Liverpool, Liverpool, UK

[5]Endoscopy Unit, Barts Health NHS Trust, The Royal London Hospital, London, UK

CORRESPONDING AUTHOR INFORMATION

David P. Kelsell (d.p.kelsell@qmul.ac.uk) ORCID: 0000-0002-9910-7144

CONFLICT OF INTEREST STATEMENT

The authors disclose no conflicts.

AUTHOR CONTRIBUTIONS TO MANUSCRIPT

SM co-wrote the manuscript/figures, analysed RNA-Seq data, and performed immunohistochemical staining. CMW, DB, HLdP, LM, and JC-C helped generate RNA-Seq data and performed tissue processing and immunohistochemical staining. RP advised on RNA-Seq analysis. PW, HLS, JKF, and JMR provided clinical expertise and human tissue biopsies. ARS, DCB, and DJP provided input into the study design and experimental methods. DPK co-designed the experiment, supervised the study, and co-wrote the manuscript.

DATA TRANSPARENCY STATEMENT

RNA Sequencing data have been deposited into Gene Expression Omnibus (GEO) and are available with GEO accession number: GSE222553

FUNDING

The study was supported by grants awarded from the Medical Research Council (MR/S009914/1) and Cancer Research UK (C7570/A19107) to DPK, MRC DTP studentship to SM, WHRI Academy Marie Curie co fund (PCOFUND-GA-2013-60876) to HLdP/DPK, and a Queen Mary Impact Fund grant to SM/DPK.

REPORTING GUIDELINES

Helsinki Declaration

ETHICAL STATEMENT

Ethical approval was provided to collect esophageal biopsies from individuals with tylosis with esophageal cancer by Northwest Haydock Research Ethics Committee (Genetic Study of Tylosis and Familial Oesophageal Cancer; REC 02/8/001), and from healthy control participants by Bromley Research Ethics Committee (Bioresource Based Studies of the Digestive System in Children and Adults; REC 15/LO/2127).

ABSTRACT (260 Words Max)

BACKGROUND AND AIMS

Survival rates for esophageal squamous cell carcinoma (ESCC) are extremely low due to the late diagnosis of most cases. An understanding of the early molecular processes that lead to ESCC may facilitate opportunities for early diagnosis, however these remain poorly defined. Tylosis with esophageal cancer (TOC) is a rare syndrome associated with a high lifetime risk of ESCC and germline mutations in *RHBDF2*, encoding iRhom2. Using TOC as a model of ESCC predisposition, this study aimed to identify early-stage transcriptional changes in ESCC development.

METHODS

Esophageal biopsies were obtained from control and TOC individuals, the latter undergoing surveillance endoscopy, and adjacent diagnostic biopsies were graded as having no dysplasia or malignancy. Bulk RNA-Seq was performed, and findings were compared with sporadic ESCC vs normal RNA-Seq datasets.

RESULTS

Multiple transcriptional changes were identified in TOC samples, relative to controls, and many were detected in ESCC. Accordingly, pathway analyses predicted an enrichment of cancer-associated processes linked to cellular proliferation and metastasis, and several transcription factors were predicted to be associated with TOC and ESCC, including negative enrichment of GRHL2. Subsequently, a filtering strategy revealed 22 genes that were significantly dysregulated in both TOC and ESCC. Moreover, Keratin 17, which was upregulated in TOC and ESCC, was also found to be overexpressed at the protein level in 'normal' TOC esophagus tissue.

CONCLUSION

Transcriptional changes occur in TOC esophagus prior to the onset of dysplasia, many of which are associated with ESCC. These findings support the utility of TOC to help reveal the early molecular processes that lead to sporadic ESCC.

Key Words: iRhom2, ESCC, Tylosis with Esophageal Cancer, RNA-Seq, Early Cancer Detection

INTRODUCTION

Most esophageal squamous cell carcinomas (ESCCs) are diagnosed late when the disease is advanced and has spread from its primary site[1]. This considerably affects prognosis and chance of survival, and stage at diagnosis remains the most important prognostic factor[2]. Yet, early-stage ESCCs rarely present with symptoms, and no screening programme for at-risk individuals, such as tobacco smokers and alcohol drinkers, exists. Accordingly, an opportunity to improve early diagnosis of ESCC may be to use biomarkers of early-stage disease, although the molecular changes underpinning early-stage disease remain poorly characterised, in part, due to a lack of useful models to identify these changes.

Tylosis with Esophageal Cancer (TOC) is a rare, autosomal dominant syndrome associated with late-onset focal non-epidermolytic palmoplantar keratoderma, germline mutations in *RHBDF2* (encoding iRhom2), and a high lifetime risk of ESCC, estimated to be 90% by 70 years[3, 4]. Additionally, *RHBDF2* mutations in TOC represent the only known genetic susceptibility that leads to ESCC with high penetrance, and TOC may therefore be a useful model to identify early carcinogenic processes in the esophagus. To date, studies into the biology of TOC have largely focused on the skin[5-7], and no molecular description of TOC esophagus exists.

iRhom2 is a highly conserved, catalytically inactive Rhomboid protease associated with an array of biological functions[8]. These include facilitating the maturation and trafficking of ADAM17, which is a sheddase of multiple ligands, including those involved in the epidermal growth factor receptor (EGFR) pathway, and inflammatory cytokines, such as tumor necrosis factor alpha (TNF-α)[9, 10]. In hyperproliferative epidermal keratinocytes, such as those isolated from TOC individuals, the shedding of ADAM17 ligands and associated EGFR signalling is increased[5, 11]. Moreover, iRhom2 associates with the stress keratin, Keratin 16[6], and is a transcriptional target for p63[7], in the keratinocyte stress response. However, the biology of iRhom2 in esophageal carcinogenesis remains largely unexplored and is of importance given the role of iRhom2 as a familial esophageal squamous cancer gene.

Genome-wide transcriptomics studies have shown great utility in revealing important aspects of disease, and the ESCC transcriptome has been well explored with microarray[12, 13], bulk RNA sequencing (RNA-Seq)[14-16], and single cell RNA-Seq[17, 18] studies. How the transcriptome is altered in pre-dysplastic and pre-malignant esophageal epithelium remains unexplored, however, and may provide insight into the biology underpinning these early stages of disease. Although to date, there have been difficulties in determining which early-stage biopsies are high risk for ESCC, impeding these types of studies.

Here, bulk RNA-Seq of early-stage TOC and normal esophageal biopsies reveals the transcriptional landscape of TOC esophagus, and bioinformatics and comparison strategies uncover similarities between TOC and sporadic ESCC. Moreover, these data provide an insight into the early-stage processes underlying sporadic ESCC and represent a springboard for future investigations using TOC as a model of early-stage esophageal disease.

MATERIALS AND METHODS (Approx. 1000 Words)

PATIENT SAMPLES

Esophageal biopsies were collected from eight UK TOC family members with confirmed *RHBDF2* mutation status (c.557 T>C, p.Ile186Thr), during surveillance endoscopy (REC 02/8/001). Pathologist reports for adjacent diagnostic biopsies taken at the same level of the esophagus were provided, and these are summarised in the Results section, Fig. 1B. Six normal esophageal biopsies were collected from two volunteers who did not have a history of esophageal disease, nor any signs of esophageal erosion and/or esophagitis during endoscopy, and details of these are described in Supp. Tab 1. (REC 15/LO/2127). Given that the normal esophageal biopsies were limited to two patients, we validated the representative clustering with an additional 8 normal patient biopsies (data not shown[19]).

BULK RNA-SEQUENCING

DATA GENERATION

Biopsies for bulk RNA-Seq were collected in RNAlater® RNA Stabilising Solution (Invitrogen), and RNA was extracted and processed by Queen Mary University of London's Genome Centre. Polyadenylated mRNAs were captured using NEBNext® Poly(A) mRNA Magnetic Isolation Module (New England BioLabs), and the NEBNext® UltraTM II Directional RNA Library Prep Kit for Illumina® (New England BioLabs) was used to create cDNA libraries, which were sequenced using the NextSeq 500 System (Illumina).

DATA PROCESSING

Paired-end FASTQ files were uploaded to the RaNA-seq server[20], and Salmon[21] was used to align files to the GRCh38 human genome to produce gene-level expression estimates. Additionally, publicly available RNA-Seq datasets were imported into RaNA-seq via their Sequence Read Archive (SRA) accession number, and gene level expression estimates were generated using Salmon as described above.

BIOINFORMATICS ANALYSES

DIFFERENTIAL GENE EXPRESSION ANALYSIS

DESeq2[22] was used to identify differentially expressed genes from raw gene-level counts. Differentially expressed genes were identified by filtering by $\log_2$ fold change, adjusted *p*-value, $\log_2$ fold change standard error, and mean normalised count (as Transcripts per Million (TPM)).

CLUSTERING AND DIMENSIONALITY REDUCTION ANALYSIS

Hierarchical clustering was performed on differentially expressed genes to limit noise from lowly expressed and/or non-variable genes, and TPM counts for these were scaled and centred, and then clustered with hclust (R Stats Package, v.4.3.1). Clustering dendrograms were visualised as part of a heatmap with the pheatmap package (v.1.0.12). To perform principal components analysis (PCA), lowly expressed genes were removed, and the prcomp function (R Stats Package, v.4.3.1) was used to scale and centre TPM counts, and to generate PCA scores. Biplots of principal component 1 (PC1) and principal component 2 (PC2) were visualised using ggplot2 (v.3.4.3).

PATHWAY ENRICHMENT ANALYSIS

Lists of differentially expressed genes were processed by the Enrichr online server[23-25], to identify enriched GO Biological Process, Cellular Component, and Molecular Function terms; BioPlanet terms; and Human Phenotype Ontology terms. Terms with a false discovery rate (FDR) < 0.05 were selected. Additionally, raw gene-level counts were normalised by variance stabilising transformation (VST) by DESeq2, and lowly expressed genes were removed prior to input into the Gene Set Enrichment Analysis (GSEA) software application (v.4.3.2)[26, 27]. GSEA was performed using the Hallmark Gene Sets database to determine enriched biological pathways. Terms with a *p*-value < 0.05 and FDR < 0.25 were selected.

TRANSCRIPTION FACTOR PREDICTION ANALYSIS

Transcription factor regulons were obtained from the curated DoRothEA R package (v.1.12.0) for human (dorothea_hs)[28]. The msviper function (VIPER R package, v.1.34.0) was used in conjunction with these regulons to calculate positively and negatively enriched transcription factors. Transcription factors with a confidence score of A – D were used as input, and those with a normalised enrichment score (NES) > 1.5 or < -1.5, and *p*-value < 0.05 were selected.

STATISTICS

Statistical tests were applied to data throughout the analysis pipeline. The differential gene expression package, DESeq2, computes adjusted *p*-values, which were used to select significant genes. TPM values were $\log_2$+1 transformed to normalise data and to avoid negative values. Two-sample *t*-tests with false discovery rate (FDR) correction were applied to data using the rstatix package (v.0.7.2), and adjusted *p*-values were displayed as significance stars on plots.

QUANTITATIVE PCR

RNA from samples used for bulk RNA-Seq were used for confirmatory quantitative PCR (qPCR) reactions. RNA was converted to cDNA using the high-capacity cDNA reverse transcription kit (ThermoFisher Scientific, catalogue number: 4368814) with supplementation of an RNase inhibitor (ThermoFisher Scientific, catalogue number: N8080119). qPCR reactions were performed in triplicate in 96-well PCR plates (Starlab, catalogue number: E1403-7700). Each well contained 10µl of TaqMan^{TM}

Gene Expression Master Mix (ThermoFisher Scientific, catalogue number: 4369510), 1µl of TaqMan^{TM} Assay (ThermoFisher Scientific, catalogue number: 4331182) for a specific gene target (Supp. Tab. 2), and 9µl of sample cDNA at 10ng/µl. GAPDH was used as a housekeeping gene, and no-template-control wells, containing 9µl of nuclease-free water in place of cDNA, were run for each TaqMan^{TM} Assay mix. Plates were centrifuged and run using a StepOnePlus^{TM} Real-Time PCR System (ThermoFisher, catalogue number: 4376598), according to manufacturer's instructions. Gene expression was calculated relative to mean C_t values for GAPDH, and to average expression values across control (normal esophagus) samples, using the $2^{-\Delta\Delta Ct}$ method.

IMMUNOFLUORESCENCE STAINING

Tissue sections were obtained from OCT-embedded frozen tissue and thawed at room temperature for ~20 minutes and washed three times with phosphate buffered saline (PBS). Sections were fixed either with 4% paraformaldehyde (PFA) or 50:50 Methanol Acetone, depending on primary antibody, for 15 minutes at room temperature, washed three times with PBS (and washed for an extra 10 minutes with PBS and 0.1% Triton, in sections fixed with 4% PFA), incubated with 5% goat serum in PBS for one hour at room temperature, and incubated overnight at 4°C with primary antibody (GRHL2, HPA004820, 1 in 100 dilution, tissue fixed with 4% PFA; Keratin 17, ab51056, 1 in 300 dilution, tissue fixed with 50:50 Methanol Acetone) diluted in 5% goat serum in PBS. The following day, sections were washed three times with PBS, incubated with goat anti-rabbit IgG Alexa Fluor^{TM} 488 secondary antibody (ThermoFisher Scientific, catalogue number: A-11008) for one hour at room temperature, washed three times with PBS, incubated with DAPI (diluted 1 in 10,000 in PBS) for 10 minutes at room temperature, washed three times with PBS, and mounted using ImmuMount (Epredia).

Sections were imaged on an upright Leica DM4000 Epi-Fluorescence Microscope, and images were quantified using Fiji software.

HEMATOXYLIN AND EOSIN STAINING

Formalin fixed paraffin embedded tissue blocks were sectioned and stained for hematoxylin and eosin by Queen Mary University of London’s Pathology Services.

DATASETS ACCESSED FOR THIS STUDY

Publicly available ESCC vs normal RNA-Seq datasets were accessed via SRA using their accession numbers; SRP008496, SRP064894, SRP133303.

DATA AVAILABILITY

Bulk RNA-Seq data have been deposited into the GEO database, with accession number: GSE222553

RESULTS

TOC ESOPHAGEAL TISSUE DISPLAYS ABNORMAL HISTOLOGICAL FEATURES PRIOR TO DYSPLASIA

‘Normal’ (pre-dysplasia) TOC esophageal tissue was found to display histological differences to *bona fide* normal esophageal tissue, including a thickened superficial layer that appeared to be keratinized, suggesting an altered keratinocyte differentiation programme and barrier function (Fig. 1A). Moreover, this hinted that the hyperactive iRhom2 mutant may drive these histological changes prior to the development of dysplasia in TOC esophageal tissue[29, 30].

To explore the molecular pathways underlying these histological changes, bulk RNA-Seq was performed. Eight esophageal biopsies were obtained from four male and four female TOC individuals with confirmed *RHBDF2* mutation status (c.557 T>C, p.Ile186Thr). Pathology reports (summarised in Fig. 1B) for adjacent diagnostic biopsies taken at the same level of the esophagus revealed that none were determined to have dysplasia or malignancy, and just three adjacent samples were graded as having hyperplasia. While biopsies assessed in this project were not the exact biopsies referred to in the pathology reports, our assumption was that their histological attributes were likely to be similar given their proximity to adjacent diagnostic biopsies and given that these patients were not recommended for further treatment or close follow-up surveillance. Moreover, given these pathology findings, it was assumed that these biopsies were likely to be pre-dysplastic, and to therefore be useful to reveal early molecular changes underpinning the development of ESCC.

THE TRANSCRIPTOME IN EARLY-STAGE TOC ESOPHAGUS DIVERGES FROM A NORMAL ESOPHAGUS STATE

Initial investigations found that several iRhom2-associated genes displayed a trend of being, or were significantly, upregulated in TOC esophagus samples, including *BIRC5* (encoding the anti-apoptotic protein, SURVIVIN), *KRT16*, *RHBDF2*, and *TP63* (Fig. 2A). Conversely, *ADAM17* gene expression was comparable to normal esophagus samples (Fig. 2A); of note, prior work has shown that ADAM17 protein activity is increased in TOC skin, rather than transcript abundance[5]. Additionally, *TP53* and *TP73* were assessed given their homology to *TP63* and links to cancer[31], however their gene expression was unaltered (Fig. 2A). Differential gene expression analysis revealed > 500 significantly altered gene transcripts between TOC and normal esophagus samples, including upregulation of *S100A7*, which has been reported to be elevated in ESCC[32], and downregulation of *ESAM* (Fig. 2B). A closer look at the protein-coding genes with the largest fold change revealed an elevation of a variety of keratin genes, including *KRT14*, *KRT10*, and the differentiation associated protein, *KRTDAP*, and was suggestive of an abnormal keratinocyte differentiation programme (Fig. 2C).

To assess for trends and similarities within the data, principal components analysis (PCA) was performed, and according to PC1 (which accounted for 33.3% of variability within the dataset), three TOC samples grouped more closely to normal samples, while the other five TOC samples grouped further away, suggesting transcriptional variation between the TOC samples (Fig. 2D). To investigate further, unsupervised hierarchical clustering was performed on 1241 differentially expressed genes, and this revealed a similar clustering pattern, where four TOC samples clustered closely to normal samples, and were termed TOC 1, and four TOC samples clustered further away and displayed an opposite pattern of gene expression and were termed TOC 2 (Fig. 2Ei). Moreover, these groupings did not correlate with age or pathology criteria, such as hyperplasia (Fig. 2Eii). Given that the expression of these 1241 genes were able to separate TOC and normal samples, these were investigated by pathway analysis, and upregulated genes (in TOC samples) were associated with protein translation pathways, and downregulated genes (in TOC samples) were associated with several signalling pathways including Interleukin-1, Interleukin-2, and EGFR1 (Fig. 2Eiii). Moreover, the latter was not expected given that we have shown elevated EGFR signalling, including ADAM17 shedding of EGF ligands, in TOC skin[5, 11], suggesting that tissue context is important to understanding TOC esophageal biology. Given that the transcriptome in the TOC 2 sample group deviated from a normal esophagus state, which may suggest progression of disease, the expression of these 1241 genes were then assessed in three, independent publicly available sporadic ESCC vs normal RNA-Seq datasets: SRP008496, SRP064894, SRP133303. Visualisation of these genes via heatmaps revealed that normal and ESCC samples clustered separately, and ESCC samples displayed a visually similar gene expression pattern to TOC 2 samples (Fig. 2Fi, Supp. Fig.1), suggesting similarity between the TOC 2 sample group and ESCC, albeit without major changes to their histology. Additionally, many of these genes were differentially expressed across all three ESCC vs normal datasets, including 118 upregulated and 154 downregulated genes (Fig. 2Fii). To investigate these shared genes as transcriptional changes of interest, pathway analysis revealed that the 118 upregulated genes were predominantly associated with cellular proliferation and cell cycle pathways, suggesting that cell turnover in TOC esophageal tissue is elevated (Fig. 2Fiii).

TRANSCRIPTIONAL ANALYSES REVEAL SKIN AND CANCER ASSOCIATED PROCESSES IN EARLY-STAGE TOC ESOPHAGUS

Gene ontology (GO) analyses of significantly upregulated genes revealed an enrichment of skin-associated pathways in TOC esophageal biopsies, including epidermis development (Fig. 3Ai), lamellar body formation (Fig. 3Aii), and serine-type peptidase activity (Fig. 3Aiii). Human phenotypes associated with these upregulated genes were pathways linked to palmoplantar keratoderma (PPK) and hyperkeratosis, which are surprising data given that these genes were identified in esophageal tissue; although, of course, PPK is part of the TOC syndrome. We then investigated which genes were driving these enrichment results, and it was found these included several keratin genes, as well as others commonly associated with skin disease (Fig. 3B). Separate pathway analyses were also carried out including gene set enrichment analysis (GSEA), which considers actual gene expression values. These revealed a positive enrichment (over-representation) of several pathways commonly associated with cancer, including those linked to cellular proliferation such as MYC targets and G2M checkpoint, angiogenesis, and epithelial mesenchymal transition, the latter being associated with invasion and metastasis (Fig. 3Ci). Moreover, negatively enriched (under-represented) GSEA pathways in TOC samples included TNF-α signalling, which again contrasts with previously published data that found this pathway to be elevated in TOC skin via the iRhom2-ADAM17 pathway[5]; as well as endocrine pathways, androgen response and estrogen response early (Fig. 3Ci). We investigated the cancer-associated pathways further by visualising the expression of their core leading-edge genes (identified by GSEA software), and it was found that these genes were almost exclusively transcriptionally elevated in the TOC 2 group of samples, while TOC 1 samples generally clustered alongside normal esophageal samples and displayed a similar expression pattern (Fig. 3Cii).

To explore which transcription factors may be facilitating these transcriptional changes, we made use of the DoRothEA suite of curated regulons, which are a catalogue of transcription factors and their gene targets[28]. To improve robustness and confidence in the output, we discarded transcription factors with a confidence score of *E*, which is DoRothEA's lowest confidence score and includes transcription factors mapped to gene targets using just one information source. These analyses predicted that different transcription factors regulated the transcriptional changes observed in TOC 1 and TOC 2 samples (Fig. 3Di and ii). Given the similarities previously identified between TOC 2 and ESCC samples, further analysis was performed on three ESCC vs normal RNA-Seq datasets (SRP008496, SRP064894, SRP133303). Common transcription factors across all datasets were identified, which revealed some similarities between TOC 2 and ESCC, including negative enrichment of genes linked to the transcription factor, GRHL2 (Fig. 3Dii and iii). Exploring further, GRHL2 was found to have reasonable gene expression, and was selected for further investigation as a transcription factor of interest. Immunofluorescence staining of GRHL2 revealed a nuclear staining pattern in normal esophagus tissue, while in TOC esophagus tissue, GRHL2 staining displayed a perinuclear pattern in papillae structures (Fig. 3E, Supp. Fig. 2). Therefore, it appears that GRHL2 can accumulate outside of the nucleus in these regions of TOC esophageal tissue and supports the bioinformatics predictions of a negative enrichment of GRHL2 target genes.

SIGNIFICANT TRANSCRIPTIONAL CHANGES ARE SHARED BETWEEN EARLY-STAGE TOC ESOPHAGUS AND SPORADIC ESCC

Considering that several of our analyses identified similarities between pre-dysplastic TOC and sporadic ESCC biopsies, we sought to identify the most significant shared transcriptional changes. To do so, a two-step filtering strategy was designed: first, to identify the most significant changes between TOC and normal esophagus samples, differential gene expression lists were filtered by $\log_2$ fold change ≥ 1.5 or ≤ -1.5, adjusted p-value < 0.1, $\log_2$ fold change standard error < 1, TPM count > 100 (averaged as mean across TOC samples when identifying upregulated genes, and across normal samples when identifying downregulated genes); and second, we aimed to filter genes that were identified in the first filtering run for differentially expressed genes that were satisfied across three sporadic ESCC vs normal RNA-Seq datasets (SRP008496, SRP064894, SRP133303), with the criteria, $\log_2$ fold change ≥ 3 or ≤ -3, adjusted p-value < 0.1 (Fig. 4A). The first part of this filtering strategy identified a list of 71 significant genes, and hierarchical clustering using expression values for these genes, separated TOC and normal esophagus samples (Fig. 4B). Moreover, heatmap visualisation showed an opposite expression pattern for these genes between TOC and normal samples, and this expression pattern was largely mirrored in sporadic ESCC vs normal RNA-Seq datasets (Fig. 4B). These 71 genes were then filtered across the three sporadic ESCC vs normal RNA-Seq datasets, revealing a suite of 22 transcriptional changes, 21 downregulated, including *CRISP3*, *IL36A*, and *PSCA*, and 1 upregulated, *KRT17* (further information regarding these genes is described in Supp. Tab. 3). Visualisation of these transcriptional changes revealed a similarity between TOC and sporadic ESCC samples (Fig. 4C) and 19 of these were subsequently investigated and validated by qPCR (Supp. Fig.3).

Moreover, some of these genes have been shown to be downregulated at the protein level in ESCC, including PSCA[33]. Given that *KRT17* was transcriptionally upregulated, it was wondered whether this could be detected at the protein level, and immunofluorescence staining for Keratin 17 was performed. A specific staining pattern localised to papillae structures was observed in normal esophagus tissue, while in TOC esophagus tissue, a diffuse and strong staining pattern was observed throughout all esophageal epithelial cell layers (Fig. 4Di), and quantification of mean fluorescence intensity across 9 TOC and 3 normal esophageal samples revealed a trend of upregulated protein expression (Fig. 4Dii). Moreover, this matches previously reported Keratin 17 staining in sporadic ESCC[34], suggesting this may be an early molecular change in esophageal epithelium.

DISCUSSION

Data presented here represent the first molecular and transcriptional description of TOC esophagus, with previous studies having focused on iRhom2 biology in the skin and TOC PPK[5-7]. Furthermore, these data may provide novel insights into the early changes that underly progression to ESCC.

Numerous transcriptional changes were identifiable in TOC esophageal biopsies that were assumed to be pre-dysplastic, relative to normal (wildtype) samples. Whilst some histological aberrations, such as a thickened superficial epithelial layer, were noticeable in TOC esophageal samples (Fig. 1A), these data show that many transcriptional changes may occur prior to dysplasia in TOC, which is considered the *bona fide* precursor lesion to ESCC, and several of these changes are also present at the level of sporadic ESCC. Moreover, this indicates that TOC may be a comparable and relevant model to study sporadic ESCC. However, it is not certain whether these changes occur in early-stage pre-dysplastic sporadic cases, as TOC individuals represent a unique ESCC-predisposition cohort, and *RHBDF2* mutations are not known to be found in sporadic ESCCs unlike other familial cancer genes; rather, the genomic loci containing *RHBDF2* is frequently deleted in ESCC[35, 36]. Considering this, our data still support using TOC to understand sporadic esophageal disease, due to the many similarities observed between TOC and sporadic ESCC (validated across three independent datasets), including gene expression changes (Fig. 2F, 4B, 4C), transcription factor predictions (Fig. 3D), and enriched pathways (Fig. 2Fiii, 3C). Further, it is not currently possible to compare the transcriptomes of TOC with sporadic very early-stage esophageal hyperplasia/dysplasia to identify common early drivers of ESCC, as early-stage ESCC datasets are not available and there are no longitudinal studies where esophageal biopsies have been taken over time before the development of dysplasia and ESCC. This is the unique aspect of studying TOC.

Moreover, replicating this type of study in the sporadic setting would conceivably be difficult to achieve, as to our knowledge, no other patient cohorts are predisposed to ESCC with the same high level of penetrance as TOC. Potential alternative ESCC-predisposition cohorts may include those who live in high-risk regions, such as Zambia[37] or areas of eastern and central Asia[1], or those linked to lifestyle risk factors, such as tobacco smoking and alcohol consumption[38]; although the risk of ESCC in these cohorts is significantly lower than the risk associated with TOC. Moreover, it would be challenging to identify pre-dysplastic sporadic samples that are considered high risk for ESCC, given that no criteria except for pathology assessment currently provides a readout for disease, and dysplasia is considered the precursor lesion for ESCC[29, 30]. Therefore, while not directly equivalent, it is suggested that TOC does represent a useful and novel cohort to understand early pre-dysplastic changes in the sporadic setting, and this is supported by data presented throughout this study.

Considering the underlying biology of the TOC esophageal epithelium, changes that might be expected in PPK and skin disease were observed, including enrichment of skin-associated pathways (Fig. 3A), upregulation of several keratin genes (Fig. 3B), and diffuse and strong staining of Keratin 17 across all esophageal epithelial cell layers (Fig. 4D). Given that TOC individuals develop a focal non-epidermolytic PPK and considering that TOC esophageal histology displays an abnormally thickened and keratinized superficial layer, these findings suggest that an abnormal keratinisation and keratinocyte differentiation programme may be present in TOC esophageal tissue and suggests there may be some similarities between these two clinical sites of disease in TOC. Moreover, these changes were apparent across all TOC samples, and did not appear to conform to the TOC 1 / 2 clustering pattern, suggesting these may be constitutive changes linked to iRhom2. Considering this, iRhom2 has previously been shown to associate with the stress keratin, Keratin 16, throughout the keratinocyte stress response[6], and given that this and other keratins have been shown to be dysregulated in esophageal epithelium, these may also be linked to iRhom2. Moreover, this suggests that iRhom2 may be a novel and key regulator of multiple keratins in epithelial tissues, and links iRhom2 to the sporadic setting, given that Keratin 17 staining in TOC esophageal tissue matches previously reported staining patterns in sporadic ESCC[34]. It is also plausible that these keratin changes may be mediated by dysregulated EGFR signalling[39], downstream of ADAM17 shedding of EGFR ligands, which is facilitated by iRhom2 transport[9, 10]. However, paradoxically, EGFR1 and TNF-α signalling were predicted to be negatively enriched in TOC esophageal samples (Fig. 2Eiii, Fig. 3C, respectively), suggesting that these observed changes are not downstream of ADAM17 shedding activity. By contrast, these processes are known to be elevated in TOC skin[5], and therefore, these data suggest that TOC and iRhom2 biology in esophageal tissue may be different to the skin and is context specific.

Other considerations include whether iRhom2 is acting to directly or indirectly mediate transcriptional changes in TOC esophageal tissue. It is known that iRhom2 is associated with p63 activity in stressed epidermal keratinocytes[7]; however, our analysis did not predict p63 gene targets to be transcriptionally dysregulated in either TOC 1 or TOC 2 (or ESCC) samples (Fig. 3D), suggesting differences between skin and esophageal tissue in TOC. One finding of interest may be the predicted negative enrichment of GRHL2 gene targets (Fig. 3Dii and iii) and the perinuclear / cytoplasmic accumulation of GRHL2 protein in papillae structures in TOC esophageal tissue (Fig. 3E). Previous work revealed that cytoplasmic localisation of a related family member, GRHL3, leads to changes in epidermal differentiation and morphogenesis[40], and it may be that cytoplasmic localisation of GRHL2 in TOC esophageal tissue drives aberrant differentiation; particularly as this staining pattern was not observed in normal esophageal tissue. Furthermore, a link between p63 and GRHL2 in maintaining a normal epithelial phenotype in keratinocytes has been reported[41], and given the link between p63 and iRhom2, we suggest this be explored with future experimentation. Also of note, recent work has found that an N-terminal fragment of iRhom2 can localise to the nucleus and mediate transcriptional changes[42]. While not explored in esophageal cells or tissue, these findings may link to data presented in this study and could aid understanding of iRhom2 function in esophageal tissue.

Additionally, 22 significant transcriptional changes were identified in TOC and sporadic ESCC samples, relative to normal esophageal samples (Fig. 4C). These data show that similar transcriptional changes are detectable in samples with limited histological pathology, underscoring TOC as a useful model of sporadic disease. While no validation has been performed using pre-dysplastic sporadic samples, these 22 transcriptional changes may be novel markers of early-stage pre-dysplastic disease, and we propose similar types of studies have potential to identify other markers of esophageal disease.

This study has compared the transcriptomes of TOC and sporadic ESCC, and provides a platform for future investigations to reveal early carcinogenic changes in the esophagus. These data also reveal potential effects of iRhom2, a novel familial esophageal cancer gene, in esophageal biology and homeostasis, and suggests tissue specific effects and previously unassigned functions for this pleiotropic protein.

1. Abnet CC, Arnold M, Wei WQ. Epidemiology of Esophageal Squamous Cell Carcinoma. Gastroenterology 2018;154:360-373.
2. Arnold M, Morgan E, Bardot A, et al. International variation in oesophageal and gastric cancer survival 2012-2014: differences by histological subtype and stage at diagnosis (an ICBP SURVMARK-2 population-based study). Gut 2022;71:1532-1543.
3. Blaydon DC, Etheridge SL, Risk JM, et al. RHBDF2 mutations are associated with tylosis, a familial esophageal cancer syndrome. Am J Hum Genet 2012;90:340-6.
4. Ellis A, Risk JM, Maruthappu T, et al. Tylosis with oesophageal cancer: Diagnosis, management and molecular mechanisms. Orphanet J Rare Dis 2015;10:126.
5. Brooke MA, Etheridge SL, Kaplan N, et al. iRHOM2-dependent regulation of ADAM17 in cutaneous disease and epidermal barrier function. Hum Mol Genet 2014;23:4064-76.
6. Maruthappu T, Chikh A, Fell B, et al. Rhomboid family member 2 regulates cytoskeletal stress-associated Keratin 16. Nat Commun 2017;8:14174.
7. Arcidiacono P, Webb CM, Brooke MA, et al. p63 is a key regulator of iRHOM2 signalling in the keratinocyte stress response. Nat Commun 2018;9:1021.
8. Chao-Chu J, Murtough S, Zaman N, et al. iRHOM2: A Regulator of Palmoplantar Biology, Inflammation, and Viral Susceptibility. J Invest Dermatol 2021;141:722-726.
9. Adrain C, Zettl M, Christova Y, et al. Tumor necrosis factor signaling requires iRhom2 to promote trafficking and activation of TACE. Science 2012;335:225-8.
10. M^{c}Ilwain DR, Lang PA, Maretzky T, et al. iRhom2 regulation of TACE controls TNF-mediated protection against Listeria and responses to LPS. Science 2012;335:229-32.
11. Wolf C, Qian Y, Brooke MA, et al. ADAM17/EGFR axis promotes transglutaminase-dependent skin barrier formation through phospholipase C γ1 and protein kinase C pathways. Sci Rep 2016;6:39780.
12. Su H, Hu N, Yang HH, et al. Global gene expression profiling and validation in esophageal squamous cell carcinoma and its association with clinical phenotypes. Clin Cancer Res 2011;17:2955-66.
13. Hu N, Clifford RJ, Yang HH, et al. Genome wide analysis of DNA copy number neutral loss of heterozygosity (CNNLOH) and its relation to gene expression in esophageal squamous cell carcinoma. BMC Genomics 2010;11:576.
14. Tong M, Chan KW, Bao JY, et al. Rab25 is a tumor suppressor gene with antiangiogenic and anti-invasive activities in esophageal squamous cell carcinoma. Cancer Res 2012;72:6024-35.
15. Zhan XH, Jiao JW, Zhang HF, et al. A three-gene signature from protein-protein interaction network of LOXL2- and actin-related proteins for esophageal squamous cell carcinoma prognosis. Cancer Med 2017;6:1707-1719.
16. Wang W, Wei C, Li P, et al. Integrative analysis of mRNA and lncRNA profiles identified pathogenetic lncRNAs in esophageal squamous cell carcinoma. Gene 2018;661:169-175.
17. Zhang X, Peng L, Luo Y, et al. Dissecting esophageal squamous-cell carcinoma ecosystem by single-cell transcriptomic analysis. Nat Commun 2021;12:5291.
18. Dinh HQ, Pan F, Wang G, et al. Integrated single-cell transcriptome analysis reveals heterogeneity of esophageal squamous cell carcinoma microenvironment. Nat Commun 2021;12:7335.

19. Ustaoglu A, Daudali FA, D'Afflitto M, et al. Identification of novel immune cell signature in gastroesophageal reflux disease: altered mucosal mast cells and dendritic cell profile. Front Immunol 2023;14:1282577.
20. Prieto C, Barrios D. RaNA-Seq: Interactive RNA-Seq analysis from FASTQ files to functional analysis. Bioinformatics 2019.
21. Patro R, Duggal G, Love MI, et al. Salmon provides fast and bias-aware quantification of transcript expression. Nat Methods 2017;14:417-419.
22. Love MI, Huber W, Anders S. Moderated estimation of fold change and dispersion for RNA-seq data with DESeq2. Genome Biol 2014;15:550.
23. Chen EY, Tan CM, Kou Y, et al. Enrichr: interactive and collaborative HTML5 gene list enrichment analysis tool. BMC Bioinformatics 2013;14:128.
24. Kuleshov MV, Jones MR, Rouillard AD, et al. Enrichr: a comprehensive gene set enrichment analysis web server 2016 update. Nucleic Acids Res 2016;44:W90-7.
25. Xie Z, Bailey A, Kuleshov MV, et al. Gene Set Knowledge Discovery with Enrichr. Curr Protoc 2021;1:e90.
26. Mootha VK, Lindgren CM, Eriksson KF, et al. PGC-1alpha-responsive genes involved in oxidative phosphorylation are coordinately downregulated in human diabetes. Nat Genet 2003;34:267-73.
27. Subramanian A, Tamayo P, Mootha VK, et al. Gene set enrichment analysis: a knowledge-based approach for interpreting genome-wide expression profiles. Proc Natl Acad Sci U S A 2005;102:15545-50.
28. Garcia-Alonso L, Holland CH, Ibrahim MM, et al. Benchmark and integration of resources for the estimation of human transcription factor activities. Genome Res 2019;29:1363-1375.
29. Wang GQ, Abnet CC, Shen Q, et al. Histological precursors of oesophageal squamous cell carcinoma: results from a 13 year prospective follow up study in a high risk population. Gut 2005;54:187-92.
30. Taylor PR, Abnet CC, Dawsey SM. Squamous dysplasia--the precursor lesion for esophageal squamous cell carcinoma. Cancer Epidemiol Biomarkers Prev 2013;22:540-52.
31. Zawacka-Pankau JE. The Role of p53 Family in Cancer. Cancers (Basel) 2022;14.
32. Lu Z, Zheng S, Liu C, et al. S100A7 as a potential diagnostic and prognostic biomarker of esophageal squamous cell carcinoma promotes M2 macrophage infiltration and angiogenesis. Clin Transl Med 2021;11:e459.
33. Zhang LY, Wu JL, Qiu HB, et al. PSCA acts as a tumor suppressor by facilitating the nuclear translocation of RB1CC1 in esophageal squamous cell carcinoma. Carcinogenesis 2016;37:320-332.
34. Liu Z, Yu S, Ye S, et al. Keratin 17 activates AKT signalling and induces epithelial-mesenchymal transition in oesophageal squamous cell carcinoma. J Proteomics 2020;211:103557.
35. Iwaya T, Maesawa C, Ogasawara S, et al. Tylosis esophageal cancer locus on chromosome 17q25.1 is commonly deleted in sporadic human esophageal cancer. Gastroenterology 1998;114:1206-10.
36. von Brevern M, Hollstein MC, Risk JM, et al. Loss of heterozygosity in sporadic oesophageal tumors in the tylosis oesophageal cancer (TOC) gene region of chromosome 17q. Oncogene 1998;17:2101-5.

37. Asombang AW, Kayamba V, Lisulo MM, et al. Esophageal squamous cell cancer in a highly endemic region. World J Gastroenterol 2016;22:2811-7.
38. Sheikh M, Poustchi H, Pourshams A, et al. Individual and Combined Effects of Environmental Risk Factors for Esophageal Cancer Based on Results From the Golestan Cohort Study. Gastroenterology 2019;156:1416-1427.
39. Jiang CK, Magnaldo T, Ohtsuki M, et al. Epidermal growth factor and transforming growth factor alpha specifically induce the activation- and hyperproliferation-associated keratins 6 and 16. Proc Natl Acad Sci U S A 1993;90:6786-90.
40. Kimura-Yoshida C, Mochida K, Nakaya MA, et al. Cytoplasmic localization of GRHL3 upon epidermal differentiation triggers cell shape change for epithelial morphogenesis. Nat Commun 2018;9:4059.
41. Mehrazarin S, Chen W, Oh JE, et al. The p63 Gene Is Regulated by Grainyhead-like 2 (GRHL2) through Reciprocal Feedback and Determines the Epithelial Phenotype in Human Keratinocytes. J Biol Chem 2015;290:19999-20008.
42. Dulloo I, Tellier M, Levet C, et al. Cleavage of the pseudoprotease iRhom2 by the signal peptidase complex reveals an ER-to-nucleus signalling pathway. bioRxiv 2022:2022.11.28.518246.

FIGURE LEGENDS

FIGURE 1. Histological summary of TOC esophageal biopsies

(**A**) Representative H&E images of normal and TOC esophagus tissue. Dotted line is drawn to indicate beginning of superficial terminally differentiated cell layer, and arrows are shown to indicate width of this tissue region. Scale = 100µm. (**B**) Pathology reports for biopsies taken at adjacent regions in the esophagus to samples processed for bulk RNA-Seq. Pathology notes were summarised according to relevant histological criteria. N = No, Y = Yes, NM = Not Mentioned.

FIGURE 2. Early-stage TOC esophageal biopsies display a gene expression profile that is distinct from a normal esophagus state and is transcriptionally similar to ESCC

(**A**) Boxplots showing expression counts (as log2(TPM+1)) in TOC and normal esophageal samples, for 7 genes associated with TOC and iRhom2. Adjusted *p*-values are shown, and statistical significance was calculated using a two-sample t-test with the rstatix package (v.0.7.2). ns – Not Significant, ***p*<0.01. Plot produced using ggplot2 (v.3.4.3). (**B**) Volcano plot showing differentially expressed genes between TOC and normal esophageal samples. Before plotting, differential gene expression matrices were filtered for genes with mean TPM count > 5. Vertical red lines indicate log2 fold change of -1 and 1, and the horizontal red line indicates an adjusted p-value of 0.1. Black points denote non-significant genes, blue points denote downregulated genes, and red points denote upregulated genes. (**C**) Bar plot showing the top 10 upregulated and top 10 downregulated genes (ranked by log2 fold change) in TOC esophagus samples, relative to normal esophagus controls. (**D**) PCA plot of PC1 and PC2, calculated using 9829 genes with mean TPM count > 5. A vertical dotted line is shown, indicating a split of samples along PC1. Principal components were calculated using base R's stats package (v.4.3.1). (**E**) (**i**) Heatmap of TPM values for 1241 differentially expressed genes (identified in TOC vs normal samples by: log2 fold change ≥ 0.58 or ≤ -0.58 (fold change of 1.5), adjusted *p*-value < 0.1, and mean TPM value > 10) in TOC vs normal samples; (**ii**) clustering dendrogram, colour-coded according to normal, TOC 1, and TOC 2 transcriptional clusters; and (**iii**) top 5 enriched BioPlanet pathways (ranked by adjusted p-value) associated with downregulated and upregulated genes used to identify the TOC 1 and TOC 2 transcriptional clusters. Heatmap produced using pheatmap package in R (v.1.0.12); dendrogram produced using hclust (R Stats Package, v.4.3.1) and visualised using dendextend (v.1.17.1) and ggplot2 (v.3.4.3); and gene ontology bar plot produced using ggplot2 (v.3.4.3). (**F**) (**i**) Heatmap of TPM values for genes identified in part Ei, in ESCC and normal samples (SRP133303). (**ii**) Euler diagrams showing how many of the 1241 genes are significantly upregulated or downregulated in ESCC samples, and how many are shared between three publicly available ESCC vs normal datasets; SRP008496, SRP064894, and SRP133303. (**iii**) Over-represented BioPlanet pathways associated with the 118 common upregulated genes in ESCC samples. Heatmap produced using pheatmap package in R (v.1.0.12); Euler diagrams produced using eulerr package in R (v.7.0.0); gene ontology bar plot produced using ggplot2 (v.3.4.3).

FIGURE 3. Pathway and transcription factor prediction analyses reveal early molecular changes in TOC that reflect PPK and ESCC

(**A**) Top 5 (ranked by adjusted p-value) over-represented Gene Ontology pathways, split by (**i**) Biological Process, (**ii**) Molecular Function, and (**iii**) Cellular Component, and (**iv**) Human Phenotype Ontology terms, associated with 88 upregulated genes in TOC esophageal samples, relative to control samples, identified by log2 fold change > 1.5, adjusted *p*-value < 0.1, log2 fold change standard error < 1, and mean TPM value across samples > 5. Bar plots produced using ggplot2 (v.3.4.3). (**B**) Boxplots showing expression counts (as log2(TPM+1)) in TOC and normal esophageal samples for 7 genes linked to the Palmoplantar Keratoderma Human Phenotype Ontology [HP:0000982], that were identified as being upregulated in TOC esophageal samples. Adjusted p-values are shown. Statistical significance was calculated using a two-sample t-test with the rstatix package (v.0.7.2). **p*<0.05 ***p*<0.01, ****p*<0.001. Plot produced using ggplot2 (v.3.4.3). (**C**) (**i**) Bar plots showing enriched GSEA hallmark gene sets (*p* < 0.05 and FDR < 0.25) in TOC esophageal samples, relative to controls. (**ii**) Heatmaps showing expression of core enriched genes associated with angiogenesis, EMT, and cell proliferation (collated across MYC Targets V1 and V2, E2F Targets, and G2M Checkpoint pathways), and colour coded according to normal, TOC 1, and TOC 2 transcriptional clusters. Beneath each heatmap, GSEA enrichment plots are shown, and the associated plot for MYC targets V2 is shown as representation for cell proliferation. Enrichment was performed using GSEA software (v.4.3.2). Significance scores are denoted as **p*<0.05, ***p*<0.01, ****p*<0.001. Plots were produced using pheatmap (v.1.0.12) and ggplot2 (v.3.4.3). (**D**) Bar plots showing NES for enriched transcription factors in (**i**) TOC1, (**ii**) TOC 2, and (**iii**) ESCC esophageal samples. Transcription factors enriched in ESCC were assessed and satisfied across SRP008496, SRP064894, and SRP133303 datasets. Predictions were calculated using the VIPER algorithm (v.1.34.0) and the human DoRothEA curated regulon, dorothea_hs (v.1.12.0), for transcription factors with confidence scores, A to D. (**E**) Representative immunofluorescence images of GRHL2 in normal and TOC esophagus tissue. GRHL2 is shown in green; DAPI nuclei stain is shown in blue; white arrows indicate examples of cytoplasmic / perinuclear staining; magnification = x40; scale bar = 25μm.

FIGURE 4. A comparison of early-stage TOC and ESCC RNA-Seq datasets reveals 22 genes that are commonly dysregulated

(**A**) Schematic describing the filtering strategy that was designed to identify significant genes and to compare TOC and ESCC RNA-Seq datasets. (**B**) Heatmaps showing TPM counts for 71 genes that were identified according to Aim 1, described in part A, in TOC and normal, and ESCC and normal (SRP133303) esophageal samples. Heatmaps produced using pheatmap (v.1.0.12). Normal samples are annotated with dark green-blue; TOC and ESCC samples are annotated with orange; genes downregulated in TOC are annotated with dark blue; and genes upregulated in TOC are annotated with green. (**C**) Boxplots showing expression counts (as log2(TPM+1)) for 22 genes identified according to Aim 2, outlined in part A, in TOC and normal, and ESCC and normal (SRP133303) esophageal samples. Adjusted *p*-values are shown, and statistical significance was calculated using a two-sample *t*-test with the rstatix package (v.0.7.2). $^*p<0.05$, $^{**}p<0.01$, $^{***}p<0.001$, $^{****}p<0.0001$. Plots were produced using ggplot2 (v.3.4.3). (**D**) (**i**) Representative immunofluorescence images of Keratin 17 in TOC and normal esophagus tissue. Keratin 17 shown in green; DAPI nuclei stain shown in blue; magnification = x20; scale bar = 50μm. (**ii**) Boxplot showing quantification of mean fluorescence intensity of Keratin 17 staining in three control and nine TOC esophagus sections, calculated using FIJI software (v.2.1.0). Statistical significance was calculated using a two-sample *t*-test with the rstatix package in R (v.0.7.2).

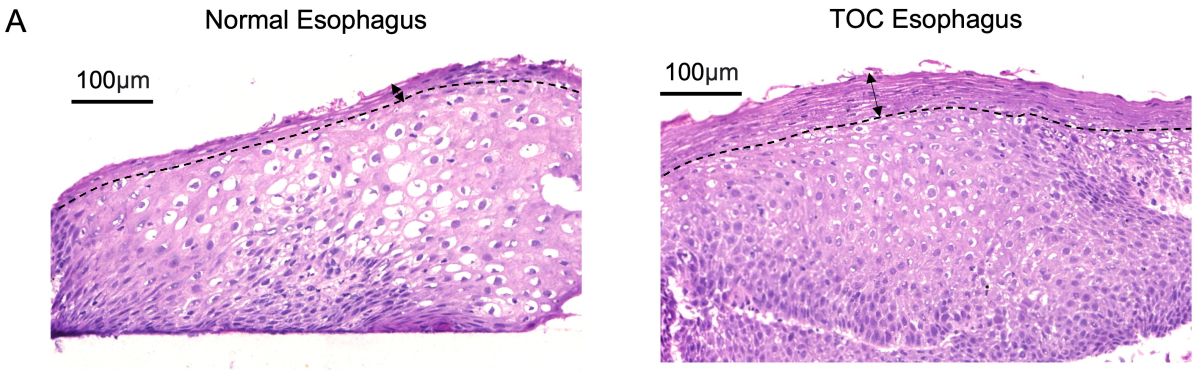

B

Sample ID	Year of Biopsy	Year of Birth	Sex	Location	Hyperplasia	Dysplasia	Malignancy
T1	2016	1949	M	31cm	NM	N	N
T2	2017	1978	M	35cm	Y (Basal Cell)	N	N
T3	2017	1946	F	35cm	NM	N	N
T4	2017	1966	M	35cm	NM	N	N
T5	2017	1971	F	33cm	Y (Mild, Basal Cell)	N	N
T6	2017	1991	F	34cm	NM	N	N
T7	2017	1994	F	34cm	Y (Mild)	N	N
T8	2017	1978	M	37cm	NM	N	N

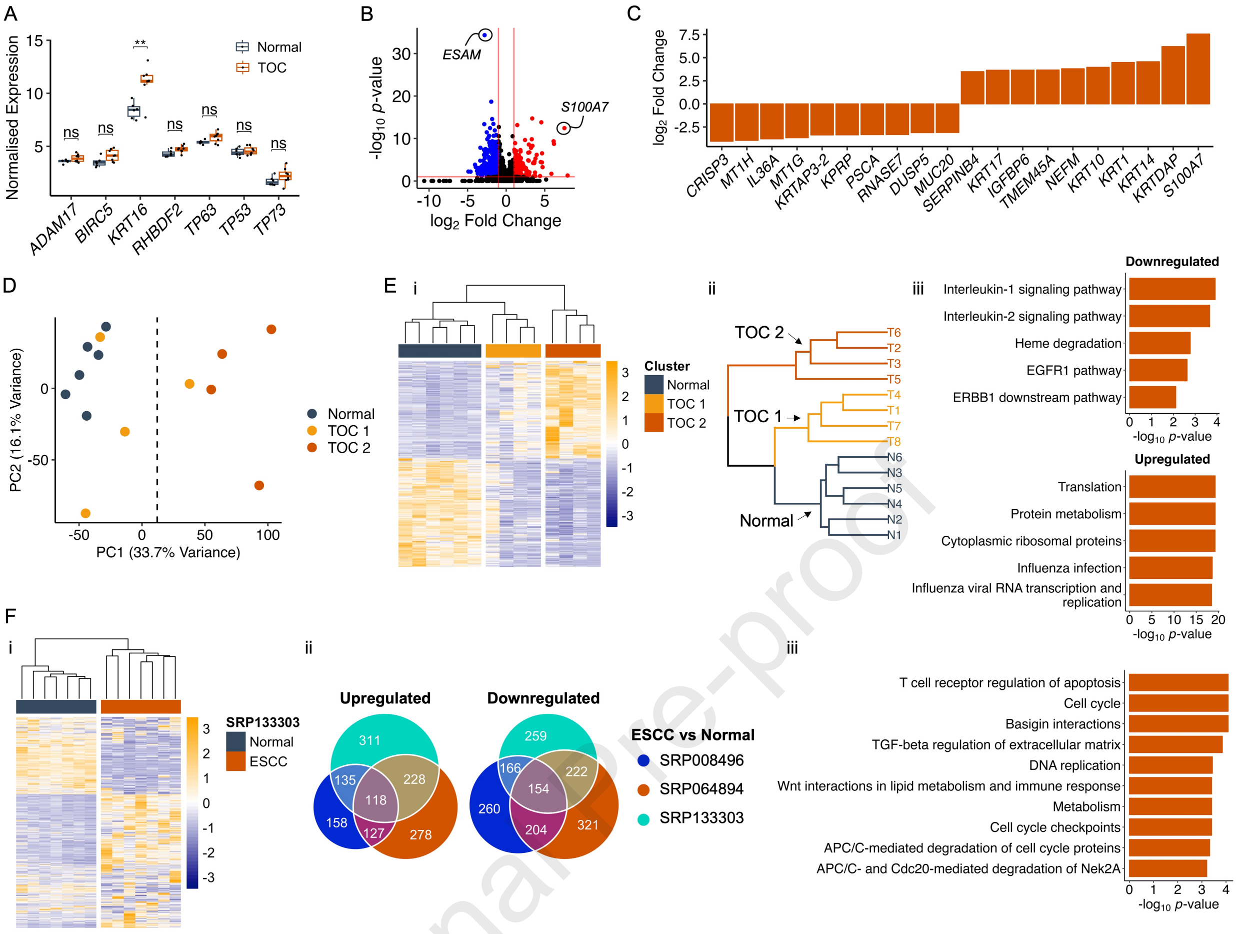
A
Normalised Expression
15
10
5
Normal
TOC
ns
ns
**
ns
ns
ns
ns
ADAM17
BIRC5
KRT16
RHBDF2
TP63
TP53
TP73
B
$-\log_{10}$ p-value
30
20
10
0
ESAM
S100A7
-10
-5
0
5
$\log_2$ Fold Change
C
$\log_2$ Fold Change
7.5
5.0
2.5
0.0
-2.5
CRISP3
MT1H
IL36A
MT1G
KRTAP3-2
KPRP
PSCA
RNASE7
DUSP5
MUC20
SERPINB4
KRT17
IGFBP6
TMEM45A
NEFM
KRT10
KRT1
KRT14
KRTDAP
S100A7
D
PC2 (16.1% Variance)
0
-50
-50
0
50
100
PC1 (33.7% Variance)
Normal
TOC 1
TOC 2
E
i
3
2
1
0
-1
-2
-3
Cluster
Normal
TOC 1
TOC 2
ii
TOC 2
TOC 1
Normal
T6
T2
T3
T5
T4
T1
T7
T8
N6
N3
N5
N4
N2
N1
iii
Downregulated
Interleukin-1 signaling pathway
Interleukin-2 signaling pathway
Heme degradation
EGFR1 pathway
ERBB1 downstream pathway
0 1 2 3 4
$-\log_{10}$ p-value
Upregulated
Translation
Protein metabolism
Cytoplasmic ribosomal proteins
Influenza infection
Influenza viral RNA transcription and replication
0 5 10 15 20
$-\log_{10}$ p-value
F
i
3
2
1
0
-1
-2
-3
SRP133303
Normal
ESCC
ii
Upregulated
311
135
228
118
158
127
278
Downregulated
259
166
222
154
260
204
321
ESCC vs Normal
SRP008496
SRP064894
SRP133303
iii
T cell receptor regulation of apoptosis
Cell cycle
Basigin interactions
TGF-beta regulation of extracellular matrix
DNA replication
Wnt interactions in lipid metabolism and immune response
Metabolism
Cell cycle checkpoints
APC/C-mediated degradation of cell cycle proteins
APC/C- and Cdc20-mediated degradation of Nek2A
0 1 2 3 4
$-\log_{10}$ p-value

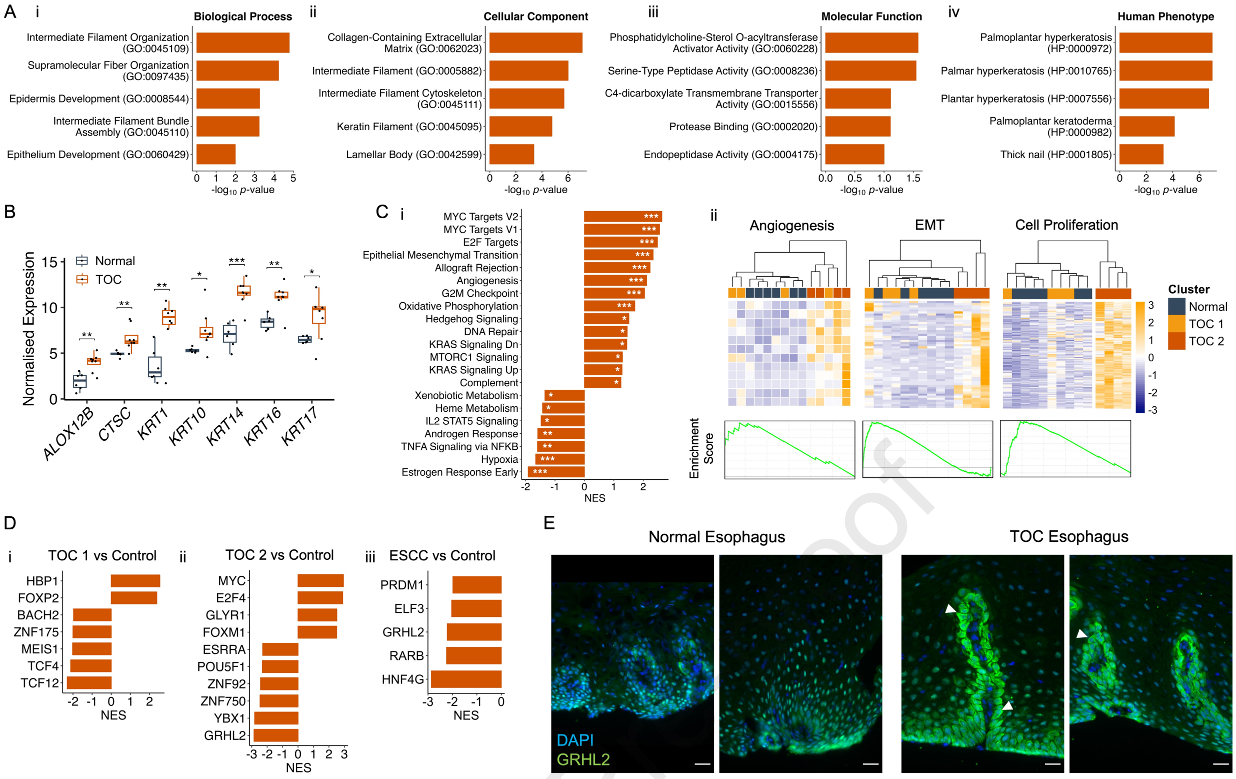
A
i
Biological Process
Intermediate Filament Organization (GO:0045109)
Supramolecular Fiber Organization (GO:0097435)
Epidermis Development (GO:0008544)
Intermediate Filament Bundle Assembly (GO:0045110)
Epithelium Development (GO:0060429)
0 1 2 3 4 5
-log10 p-value
ii
Cellular Component
Collagen-Containing Extracellular Matrix (GO:0062023)
Intermediate Filament (GO:0005882)
Intermediate Filament Cytoskeleton (GO:0045111)
Keratin Filament (GO:0045095)
Lamellar Body (GO:0042599)
0 2 4 6
-log10 p-value
iii
Molecular Function
Phosphatidylcholine-Sterol O-acyltransferase Activator Activity (GO:0060228)
Serine-Type Peptidase Activity (GO:0008236)
C4-dicarboxylate Transmembrane Transporter Activity (GO:0015556)
Protease Binding (GO:0002020)
Endopeptidase Activity (GO:0004175)
0.0 0.5 1.0 1.5
-log10 p-value
iv
Human Phenotype
Palmoplantar hyperkeratosis (HP:0000972)
Palmar hyperkeratosis (HP:0010765)
Plantar hyperkeratosis (HP:0007556)
Palmoplantar keratoderma (HP:0000982)
Thick nail (HP:0001805)
0 2 4 6
-log10 p-value
B
Normal
TOC
Normalised Expression
0 5 10 15
** ** ** * *** ** *
ALOX12B CTSC KRT1 KRT10 KRT14 KRT16 KRT17
C i
MYC Targets V2 ***
MYC Targets V1 ***
E2F Targets ***
Epithelial Mesenchymal Transition ***
Allograft Rejection ***
Angiogenesis ***
G2M Checkpoint ***
Oxidative Phosphorylation ***
Hedgehog Signaling *
DNA Repair *
KRAS Signaling Dn *
MTORC1 Signaling *
KRAS Signaling Up *
Complement *
Xenobiotic Metabolism *
Heme Metabolism *
IL2 STAT5 Signaling *
Androgen Response **
TNFA Signaling via NFKB **
Hypoxia ***
Estrogen Response Early ***
-2 -1 0 1 2
NES
ii
Angiogenesis
EMT
Cell Proliferation
Enrichment Score
3 2 1 0 -1 -2 -3
Cluster
Normal
TOC 1
TOC 2
D
i TOC 1 vs Control
HBP1
FOXP2
BACH2
ZNF175
MEIS1
TCF4
TCF12
-2 -1 0 1 2
NES
ii TOC 2 vs Control
MYC
E2F4
GLYR1
FOXM1
ESRRA
POU5F1
ZNF92
ZNF750
YBX1
GRHL2
-3 -2 -1 0 1 2 3
NES
iii ESCC vs Control
PRDM1
ELF3
GRHL2
RARB
HNF4G
-3 -2 -1 0
NES
E
Normal Esophagus
TOC Esophagus
DAPI
GRHL2

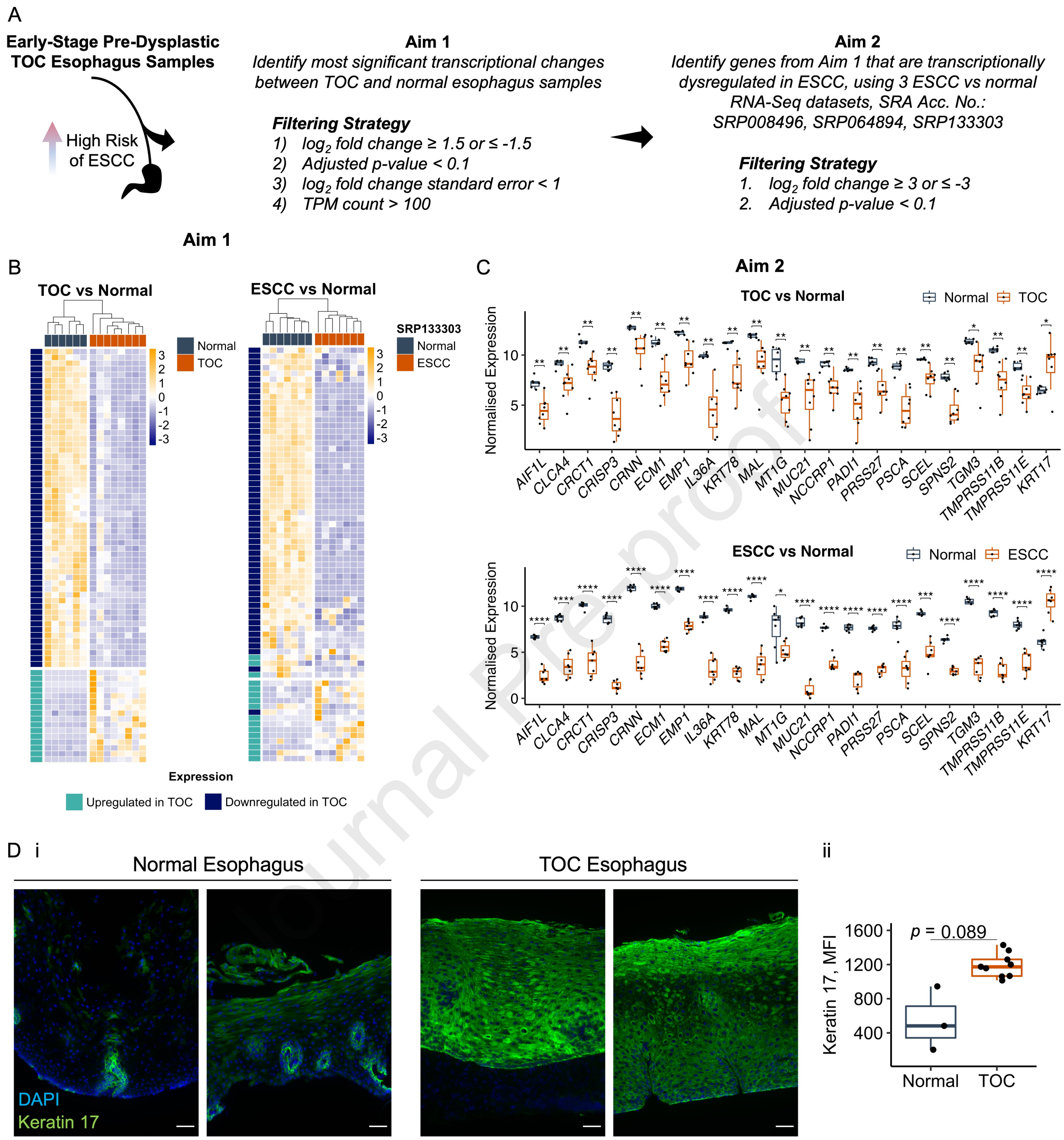
A
Early-Stage Pre-Dysplastic TOC Esophagus Samples
High Risk of ESCC
Aim 1
Identify most significant transcriptional changes between TOC and normal esophagus samples
Filtering Strategy
1) $\log_2$ fold change ≥ 1.5 or ≤ -1.5
2) Adjusted p-value < 0.1
3) $\log_2$ fold change standard error < 1
4) TPM count > 100
Aim 2
Identify genes from Aim 1 that are transcriptionally dysregulated in ESCC, using 3 ESCC vs normal RNA-Seq datasets, SRA Acc. No.: SRP008496, SRP064894, SRP133303
Filtering Strategy
1. $\log_2$ fold change ≥ 3 or ≤ -3
2. Adjusted p-value < 0.1
Aim 1
B
TOC vs Normal
Normal
TOC
3 2 1 0 -1 -2 -3
ESCC vs Normal
SRP133303
Normal
ESCC
3 2 1 0 -1 -2 -3
Expression
Upregulated in TOC
Downregulated in TOC
C
Aim 2
TOC vs Normal
Normal TOC
Normalised Expression
10
5
AIF1L CLCA4 CRCT1 CRISP3 CRNN ECM1 EMP1 IL36A KRT78 MAL MT1G MUC21 NCCRP1 PADI1 PRSS27 PSCA SCEL SPNS2 TGM3 TMPRSS11B TMPRSS11E KRT17
ESCC vs Normal
Normal ESCC
Normalised Expression
10
5
0
AIF1L CLCA4 CRCT1 CRISP3 CRNN ECM1 EMP1 IL36A KRT78 MAL MT1G MUC21 NCCRP1 PADI1 PRSS27 PSCA SCEL SPNS2 TGM3 TMPRSS11B TMPRSS11E KRT17
D i
Normal Esophagus
TOC Esophagus
DAPI
Keratin 17
ii
Keratin 17, MFI
1600
1200
800
400
p = 0.089
Normal TOC